

Modeling receptive-field structure of koniocellular, magnocellular, and parvocellular LGN cells in the owl monkey (*Aotus trivigatus*)

XIANGMIN XU,¹ A.B. BONDS,² AND VIVIEN A. CASAGRANDE^{1,3,4}

¹Department of Psychology, Vanderbilt University, Nashville

²Department of Electrical Engineering & Computer Science, Vanderbilt University, Nashville

³Department of Cell and Developmental Biology, Vanderbilt University, Nashville

⁴Department of Ophthalmology & Visual Sciences, Vanderbilt University, Nashville

(RECEIVED March 25, 2002; ACCEPTED September 5, 2002)

Abstract

Most cells in the retina and lateral geniculate nucleus (LGN) of primates have a concentric center/surround receptive-field organization. Details of the relationship between center and surround often can be used to predict how cells respond to visual stimuli. Models of the receptive-field organization and center/surround relationships also are useful when comparing cell classes. In the present study, we used the difference-of-Gaussians (DOG) model to quantitatively examine and compare the receptive-field center/surround organization of koniocellular (K), magnocellular (M), and parvocellular (P) LGN cells of owl monkeys. We obtained estimates of receptive-field center size (r_c) and center sensitivity (K_c), and surround size (r_s), and surround sensitivity (K_s) from 62 K, M, and P LGN cells by fitting their spatial-frequency responses with a DOG function (Rodieck, 1965; Croner & Kaplan, 1995). The DOG function not only accounted for the responses of P and M cells, but also provided a good description of K-cell responses. We found that at matched eccentricities of less than 15 deg, K cells had the largest r_c and r_s among the three cell classes. K cells also had the lowest K_c and K_s . Center and surround sizes tended to increase with retinal eccentricity for all three cell classes, but K cells showed a more variable pattern. There was an inverse relationship between sensitivity and size for both the receptive-field center and surround in all three cell classes. The surround/center volume ratio remained similar across cell classes. We conclude that K, M, and P LGN cell classes differ in the details of their receptive-field structure, but share common principles of center/surround organization.

Keywords: Difference of Gaussians, Primate, Vision, Thalamus

Introduction

The difference-of-Gaussians (DOG) model has been employed commonly as a mathematical description of spatial receptive fields of retinal ganglion cells and lateral geniculate nucleus (LGN) cells in the visual system (see Irvin et al., 1993; Croner & Kaplan, 1995; White et al., 2001). A large amount of information regarding receptive-field dimensions and organization has come from this compact yet accurate modeling approach (cats: Rodieck, 1965; Enroth-Cugell & Robson, 1966; So & Shapley, 1981; Linsenmeier et al., 1982; Rowe & Cox, 1993; tree shrews: Norton et al., 1989; macaque monkeys: Derrington & Lennie, 1984; Croner & Kaplan, 1995; bush babies: Norton et al., 1988; Irvin et al., 1993; owl monkeys: O'Keefe et al., 1998; marmosets: Kremers & Weiss,

1997; White et al., 2001). This approach can quantitatively address the relative strengths and sizes of center and surround mechanisms and characterize the receptive-field center/surround relationships of retinal ganglion cells and LGN cells. DOG models have proved useful in suggesting mechanisms to explain how cells respond to visual stimuli (Rodieck, 1965; Enroth-Cugell & Robson, 1966; Irvin et al., 1993). Such quantitative modeling also is useful when comparing cell classes and providing fundamental explanations for their physiology and functional roles.

The primate visual system processes different aspects of visual information in parallel. The koniocellular (K), magnocellular (M), and parvocellular (P) pathways project from the retina *via* separate layers of the LGN to primary visual cortex (V1) (Casagrande & Norton, 1991; Casagrande, 1994; Hendry & Reid, 2000). These LGN cell classes are morphologically and physiologically distinct. A number of investigators have proposed that each pathway plays a different role in vision based upon different connections and receptive-field properties (see Casagrande, 1994; Hendry & Reid, 2000; Xu et al., 2001a for reviews).

Address correspondence and reprint requests to: Vivien A. Casagrande, Department of Cell and Developmental Biology, Vanderbilt Medical School, Medical Center North B2323, Nashville, TN 37232-2175, USA. E-mail: vivien.casagrande@mcmail.vanderbilt.edu

Although the receptive-field structure and organization of primate P and M cells has been described in detail and modeled using DOG models (e.g. Derrington & Lennie, 1984; Croner & Kaplan, 1995; Kremers & Weiss, 1997; O'Keefe et al., 1998), less effort has been devoted to quantitatively characterizing the receptive-field structure of primate LGN K cells (bush babies: Norton et al., 1988; Irvin et al., 1993; marmosets: White et al., 2001). K cells have been examined in detail in only two simian primates, the diurnal marmoset and the nocturnal owl monkey (Martin et al., 1997; White et al., 1998; White et al., 2001; Xu et al., 2001a, 2002). In marmosets, K LGN cells are the only cells that carry S cone signals (Martin et al., 1997; White et al., 1998). K cells cannot carry S cone signals in owl monkeys since S cones do not exist in these primates; owl monkeys have only a single mid-wavelength cone and are presumably color blind (Wikler & Rakic, 1990; Jacobs et al., 1993). Therefore, it becomes of interest to know whether the structure of K-cell receptive fields differs among primates depending upon their lifestyle. The structure of LGN receptive fields in owl monkeys are of additional interest since this species has been used extensively as a model in studies of visual system organization (see Casagrande & Kaas, 1994). The objective of this study was to use the DOG model to examine the receptive-field structure of K, M, and P cells in the owl monkey and compare the receptive-field organization of these three LGN cell classes to the organization of presumed homologous cell classes in other species.

Some of the findings reported here were published previously in abstract form (Xu et al., 2001b).

Materials and methods

Data acquisition

Physiological data used in the present modeling study were obtained in a related set of studies (Xu et al., 2001a, 2002) in which standard extracellular recording techniques were used to record from LGN neurons in paralyzed and anesthetized owl monkeys. All monkeys were handled and cared for according to the National Institutes of Health Guide for the Care and Use of Animals under an approved protocol from the Vanderbilt University Animal Care and Use Committee. Details of the experimental procedures including animal surgery, recording, and visual stimulation are provided in an earlier paper (Xu et al., 2001a) and are described briefly below.

Paralysis and anesthesia were maintained by intravenous infusion of vecuronium bromide ($0.2 \text{ mg} \cdot \text{kg}^{-1} \cdot \text{h}^{-1}$) and sufentanil citrate (Sufenta: $12\text{--}15 \text{ } \mu\text{g} \cdot \text{kg}^{-1} \cdot \text{h}^{-1}$) mixed in 5% dextrose lactated Ringer's delivered at a rate of 2.7 ml/h. To ensure that adequate levels of anesthesia were maintained throughout the experiment, heart rate, CO_2 levels, and electroencephalogram (EEG) activity were monitored continuously after paralysis. Pupils were dilated with atropine eye-drops (1% ophthalmic atropine sulfate). Individually fitted, clear, gas-permeable contact lenses were used to bring the retina in focus with the viewing screen located at 57 cm in front of the monkey. In some animals, lenses with 3.0-mm artificial pupils were used. No differences were seen in spatial and temporal properties of cells between monkeys in which artificial pupils were used and those in which they were not used.

We initially mapped the receptive-field boundaries and ocular dominance of each cell using manually controlled stimuli displayed on a tangent screen. During the experiment, we used visual stimuli consisting of achromatic drifting sine-wave and counter-

phase gratings presented at different spatial and temporal frequencies, contrasts, orientations, and phases in the case of counterphase gratings, presented on a CRT screen that subtended an angle of 10 deg with a background luminance of 110 cd/m^2 . This level is likely to be in the photopic range for these animals. Commercially available Parylene-coated tungsten electrodes (FHC Inc., Bowdoinham, ME) with an impedance of 5–10 M Ω were used to record from the LGN cells. Data were collected and data analysis was achieved primarily through construction of 2-s, 128 bin/s post-stimulus time histograms (PSTHs). The PSTHs for each cell were Fourier transformed and subsequently analyzed. The following receptive-field properties were measured for each cell: spatial and temporal tuning, contrast response, and linearity of spatial summation. Spatial and temporal properties of the LGN cells in the owl monkey were reported earlier (see Xu et al., 2001a, 2002).

Modeling analysis and curve fitting

The main data used for modeling in this study were the responses of LGN cells to sine-wave gratings presented at a range of spatial frequencies (0.1–12 cycles/deg), tested at optimal temporal frequencies with a 28% contrast at a single orientation (90 deg). The moderate contrast of the gratings was within each cell's quasilinear response range (See Xu et al., 2001a).

Retinal and LGN cell responses to gratings of moderate contrast are well described by a difference-of-Gaussians (DOG) equation (Rodieck, 1965; Enroth-Cugell & Robson, 1966; So & Shapley, 1981; Croner & Kaplan, 1995; Kremers & Weiss, 1997; White et al., 2001). We, therefore, fit each cell's spatial-frequency response with a DOG function as modified by Croner and Kaplan (1995):

$$R(\nu) = R_c - R_s = C [K_c \pi r_c^2 \exp[-(\pi r_c \nu)^2] - K_s \pi r_s^2 \exp[-(\pi r_s \nu)^2]],$$

where $R(\nu)$ represents the cell's response amplitude (spikes s^{-1}) at various spatial frequencies, ν ; R_c and R_s are the responses of center and surround mechanisms; C is the stimulus contrast used; r_c and r_s are the radii (in degrees) of the center and surround mechanisms at which the sensitivity of each mechanism reaches $1/e$ of the peak sensitivity value; and K_c and K_s are the peak sensitivity values (spikes $\text{s}^{-1} \text{ %contrast}^{-1} \text{ deg}^{-2}$) of the center and surround mechanisms. This model assumes that the spatial-sensitivity profiles across the center and surround regions of an LGN cell receptive field can be fit with two Gaussian functions: a narrow, high-amplitude Gaussian describing the center, and a broader, lower amplitude Gaussian describing the surround. The responses at each point in the receptive field are given by the difference between the responses of the center and surround mechanisms at that point, with the response amplitude of each mechanism determined by a Gaussian spatial-sensitivity profile.

Custom programs were written with IGOR 3.1 software (WaveMetrics, Inc., Lake Oswego, OR) to fit the DOG equation to the cell's spatial-frequency response data. Cell response amplitude scaled by stimulus contrast was defined as "sensitivity to contrast" (spikes $\text{s}^{-1} \text{ % contrast}^{-1}$), which is proportional to contrast sensitivity when responses are measured within a cell's linear response range. We plotted the sensitivity to contrast as a function of spatial frequency for each cell. We weighted the fitting using the inverse of the standard deviations of the data points. The best-

fitting parameters, K_c , r_c , K_s , and r_s , were derived from curve fits with least-squares minimization, which provided an estimate of the size and sensitivity of the center and surround components of the receptive field. As reported in previous studies (e.g. Linsenmeier et al., 1982; Norton et al., 1988; Irvin et al., 1993), only one combination of the four parameters yielded a satisfactory fit with minimum error.

Cell classification

K, M, and P cells were primarily identified based upon histological reconstructions. The depth shown on the microdrive indicated the position of each recorded cell. At least two electrolytic lesions ($5 \mu\text{A} \times 5 \text{ s}$) were made to mark the location of each electrode track to aid in reconstruction of cell locations. Using methods described in detail earlier (Xu et al., 2001a), the laminar location of each cell in the LGN was reconstructed from serial sections. The sections were stained alternately for Nissl bodies and cytochrome oxidase to show the M and P LGN layers, and immunostained for calbindin-28kD to reveal the K LGN cells.

Statistical comparison

Statistical comparisons of receptive-field parameters derived from modeling analysis across the K, M, and P groups were done by one-way ANOVA with *post hoc* mean difference tests (Tukey tests). Alpha levels of ≤ 0.05 were considered significant.

Results

We examined receptive-field properties of K, M, and P LGN cells in owl monkeys in previous studies (Xu et al., 2001a, 2002). Most P and M cells exhibit a standard center/surround organization. Overall, K cells are more heterogeneous in receptive-field organization than M and P cells, in that some K cells exhibit typical center/surround receptive fields, either ON-center with an OFF surround or the converse, while other K cells have either strong suppressive surrounds, ON-OFF surrounds, or no clear surrounds (Xu et al., 2001a). In the present study, we restricted our analysis to 68 LGN cells that responded well to grating stimuli at a moderate contrast (i.e. 28%), including 22 K cells (17 ON-center, 5 OFF-center), 21 M cells (19 ON-center, 2 OFF-center), and 25 P cells (16 ON-center, 9 OFF-center). Sixty-one out of the 68 LGN cells had standard center/surround receptive-field structures; the remaining seven cells had unclear surrounds or suppressive surrounds (3 K, 2 M, and 2 P cells). All of the K, M, and P cells showed linearity of spatial summation.

Goodness of fit of the model

The large majority of cell responses to different spatial frequencies (20 K, 20 M, & 22 P) were well fit with the DOG model equation. Nevertheless, the responses of six LGN cells (2 K, 1 M, & 3 P cells) were not well fit by the DOG model, mostly due to their multip peaked spatial-frequency response functions and/or strong low-pass tuning curves.

Fig. 1 shows examples of DOG best-fitting curves of individual K-, M-, and P-cell responses. K, M, and P cells exhibit good sensitivity to contrast over a range of spatial frequencies; M cells, however, tend to exhibit more of a low-pass curve in comparison to P and K cells.

Receptive-field shape did not appear to affect goodness of fit to the DOG model since some LGN cells in our sample were orientation sensitive with elongated fields yet still were well-fit by the model. Although Linsenmeier et al. (1982) reported that the DOG function allows for a better description for cat X cells than for Y cells in terms of goodness of fit, we did not find any significant differences in the degree of fit between the K, M, and P cell classes.

Center and surround organization

For each cell of all three LGN cell classes, the surround radius (r_s , in deg) was always larger than the center radius (r_c), and the center peak sensitivity (K_c , in spike $\text{s}^{-1} \% \text{ contrast}^{-1} \text{ deg}^{-2}$) was always larger than the surround peak sensitivity (K_s). The r_c and r_s varied with eccentricity (see below). Within the eccentricities measured (2.5–28.5 deg), the r_c for the K cells ranged in radius from 0.08 deg to 0.86 deg (median 0.29 deg), the r_c for M cells ranged from 0.06 deg to 0.78 deg (median 0.18 deg), and the r_c for P cells ranged from 0.06 deg to 0.83 deg (median 0.11 deg). The r_s for K cells ranged from 0.4 deg to 1.8 deg (median 0.84 deg), the r_s for M cells from 0.24 deg to 2.05 deg (median 0.83 deg), and the r_s for P cells from 0.27 deg to 1.67 deg (median 0.66 deg).

The mean values of the best-fitting parameters of the DOG function for the 14 K, 15 M, and 11 P cells at eccentricities of less than 15 deg are summarized in Table 1. At these matched eccentricities, K cells generally had a larger r_c and r_s than either M or P cells; and P cells had the smallest r_c and r_s . Between-group comparisons indicated that there was a significant difference among the K, M, and P cells in r_c ($P = 0.002$, one-way ANOVA). The *post hoc* tests showed that the K cells differed significantly both from the M cells ($P = 0.018$, Tukey) and from the P cells ($P = 0.002$) in r_c , although the r_c of P cells was not significantly different from that of M cells ($P = 0.512$). There was also a significant difference among the K, M, and P cells in r_s ($P = 0.036$). K cells were significantly different from P cells ($P = 0.027$), but not from M cells ($P = 0.47$) in r_s . P and M cells did not differ significantly from each other in r_s ($P = 0.25$).

K_c differed among the K, M, and P cells ($P = 0.01$). K_c was significantly different between K cells and P cells, but not between K cells and M cells (K vs. P, $P = 0.008$; K vs. M, $P = 0.523$); M and P cells did not differ significantly from each other (M vs. P, $P = 0.084$). K, M, and P cells did not differ significantly in K_s ($P = 0.17$).

The mean ratios of K_c/K_s and r_s/r_c tended to be greater for M and P cells than for K cells, although this did not reach statistical significance (K_c/K_s : $P = 0.18$; r_s/r_c : $P = 0.16$).

Receptive-field size and sensitivity

There is an inverse relationship between sensitivity (K_c and K_s) and size (r_c and r_s) for both the center and surround mechanisms (Linsenmeier et al., 1982; Derrington & Lennie, 1984; Irvin et al., 1993; Croner & Kaplan, 1995; White et al., 2001). We confirmed this trend in owl monkey LGN for all cell classes.

Fig. 2A demonstrates the relationship of K_c to r_c in K, M, and P LGN cells. On a double logarithmic scale, the K-, M-, and P-cell individual regression lines differ. The slope of the K-cell regression line lies between those of the M and P cells. The slope of the average regression line for all three cell classes was -1.29 on a log-log scale ($r^2 = 0.65$, $P < 0.0001$), which is similar to that reported for cat X and Y cells (slope: -1.23 , Linsenmeier et al.,

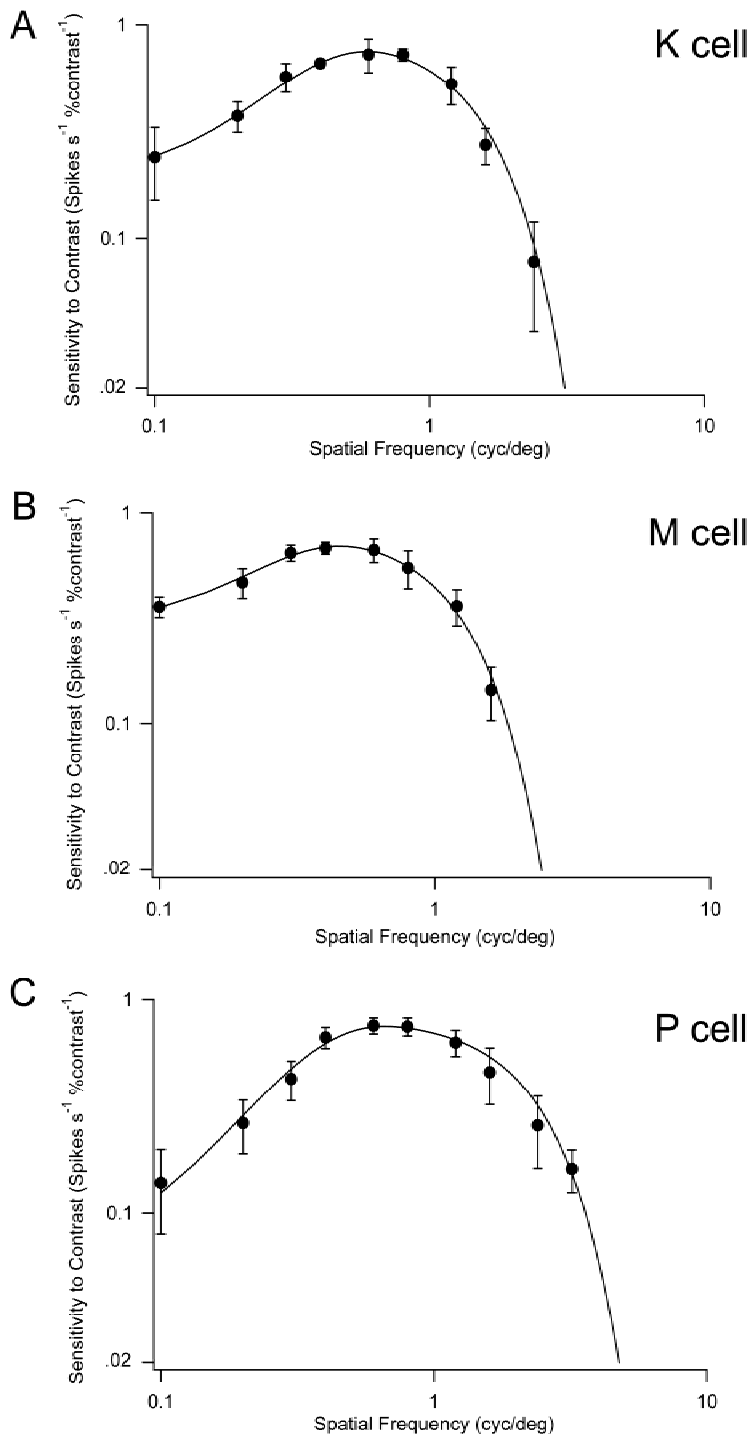


Fig. 1. Difference-of-Gaussians (DOG) functions for K, M, and P cells. LGN cell responses to achromatic drifting gratings of different spatial frequencies were collected at their optimal temporal frequency with a 28% contrast at a single orientation (90 deg). For each cell, response amplitude scaled by stimulus contrast (28%) gives sensitivity to contrast, plotted as a function of spatial frequency. Filled circles represent the cell responses. Error bars show one standard deviation above and below each response. The solid line represents the best fit of the DOG model to the cell's responses. (A) The fitted parameters for an ON-center K cell (eccentricity: 9.8 deg) are $K_c = 7.20$, $r_c = 0.20$, $K_s = 0.27$, and $r_s = 0.92$. (B) The fitted parameters for an OFF-center M cell (eccentricity: 13.5 deg) are $K_c = 4.15$, $r_c = 0.25$, $K_s = 0.12$, and $r_s = 1.18$. (C) The fitted parameters for an ON-center P cell (eccentricity: 14 deg) are $K_c = 15.80$, $r_c = 0.13$, $K_s = 0.26$, and $r_s = 0.96$.

1982) and for K, M, and P LGN cells in bush babies (slope: -1.25 , Irvin et al., 1993), but is a little less than that for the P and M cells in macaque monkeys (slope: -1.92 , Croner & Kaplan, 1995) and for the K, M, and P cells in marmosets (slope: -1.58 , White et al., 2001).

Fig. 2B suggests that the inverse relationship between sensitivity and size also holds for the surround for all three cell classes. On a double logarithmic scale, the individual regression lines of K, M, and P cells are more similar in Fig. 2B than in Fig. 2A. Their average regression line had a slope of -1.52 ($r^2 = 0.41$, $P <$

0.0001) on the log-log scale. The relationship of surround sensitivity to surround size was steeper than that of center sensitivity to center size.

Fig. 2C shows the relation of center and surround sensitivity to center and surround radius within individual cells by plotting the K_c/K_s versus r_c/r_s for each cell on a logarithmic scale. The sensitivity change between center and surround was well described by a regression line with a slope of -2.07 ($r^2 = 0.97$, $P < 0.0001$). That is, the sensitivity reduction also holds for the relationship between center and surround within individual cells.

Table 1. Average values of the best-fitting parameters of the DOG function for K, M, and P cells with eccentricities < 15 deg^a

	K_c	r_c	K_s	r_s	K_c/K_s	r_s/r_c
K cell ($n = 14$)	5.33 ± 1.76	0.31 ± 0.05	0.49 ± 0.21	0.91 ± 0.10	19.16 ± 4.28	3.61 ± 0.45
M cell ($n = 15$)	8.24 ± 1.58	0.18 ± 0.01	0.92 ± 0.59	0.77 ± 0.09	37.04 ± 12.51	4.59 ± 0.55
P cell ($n = 11$)	14.48 ± 2.70	0.12 ± 0.02	0.71 ± 0.28	0.56 ± 0.06	56.79 ± 22.10	4.59 ± 0.55

^aAverage values are mean \pm SE. K_c and K_s are in units of spikes s⁻¹ %contrast⁻¹ deg⁻²; r_c and r_s are in units of degrees of visual angle.

The relation of r_c and r_s to retinal eccentricity

Figs. 3A and 3B show the relationship between center and surround size (radius) and retinal eccentricity, respectively. Fig. 3A shows that the r_c of all cell groups increases with retinal eccentricity. The K-cell regression line had a steeper slope than that of either M or P cells, although K cells showed a more scattered pattern. P cells had a lower regression slope than M cells. In fact, the regression line of M cells was about twice as steep as that of P cells.

As shown in Fig. 3B, r_s of all cell classes tends to increase with eccentricity. Comparison with Fig. 3A indicates that the surround size of all cell classes is larger than their center size at a given eccentricity. The relationship between the M and P cell surround size and retinal eccentricity was strong and significant (M: $r^2 = 0.62$, $P = 0.002$; P: $r^2 = 0.71$, $P < 0.0001$); however, the relationship between the K cell surround size and the eccentricity was weak and nonsignificant ($r^2 = 0.24$, $P = 0.09$).

Integrated center and surround strength

If we consider the way visual cells with a concentric center/surround organization respond to visual stimuli, a key factor is the integrated strength of the surround (or the surround volume, $K_s \pi r_s^2$) in relation to the integrated strength of the center (or the center volume, $K_c \pi r_c^2$) (Enroth-Cugell & Robson, 1966; Irvin et al., 1993; Croner & Kaplan, 1995).

Fig. 4A shows that the relationship between the surround volume and the center volume for the K, M, and P cells was strong and significant ($r^2 = 0.95$, $P < 0.0001$). Only one cell (a K cell) was above the 1:1 relationship line, indicating that its surround volume was larger than its center volume. For all other K cells and all of the M and P cells, center volumes were larger than surround volumes.

In our sample, we found that K cells had significantly larger center and surround volumes (center volume: 0.83 ± 0.17 (mean \pm SE) spikes s⁻¹ %contrast⁻¹, surround volume: 0.69 ± 0.16 spikes s⁻¹ %contrast⁻¹) than P cells (center volume: 0.35 ± 0.05 , surround volume: 0.26 ± 0.04) ($P = 0.007$, one-way ANOVA; Tukey tests, $P < 0.01$ for both center and surround), although K cells did not differ significantly from M cells (center volume: 0.62 ± 0.07 , surround volume: 0.46 ± 0.05) in center and surround volume ($P = 0.35$ and 0.23). And M and P cells tended to differ in average center or surround volume, but this trend did not reach significance ($P = 0.16$ and 0.32), perhaps due to the sample size. O'Keefe et al. (1998) fitted the spatial-frequency responses of owl monkey M and PLGN cells with a different form of the best-fitting difference-of-Gaussians function and reported that M cells have significantly higher center strength and relative surround strength than P cells.

We also found that the surround/center volume ratio remained similar across all three cell classes. The surround/center volume ratio for the K cells ranged from 0.50 to 1.14 with a median of 0.77. For the M cells, the ratio ranged from 0.53 to 0.93 with a median of 0.75. The P cells' ratio ranged from 0.48 to 0.93 with a median of 0.75. Surround/center volume ratios did not differ significantly among cell classes ($P = 0.21$, one-way ANOVA).

The ratio of surround volume/center volume appears to be independent of receptive-field location for all cell classes, as Fig. 4B shows no obvious relationship exists between the ratios of center volume/surround volume and eccentricity.

Discussion

The major goal of the present study was to use quantitative modeling techniques to examine and compare the receptive-field center/surround organization of owl monkey LGN cells. The DOG function accounts for the responses of most K, M, and P cells. The model poorly fit only cells with multi-peaked or strongly low-pass spatial-frequency response functions. In the discussion below, we compare the differences between the receptive-field structures of owl monkey K, M, and P cells with those described for LGN cell classes of other species, and relate these differences to physiological properties of these cell classes. We also consider the common rules that govern the center/surround relationships of LGN cells in all classes. Finally, we briefly address the role of K cells in terms of our modeling results.

Receptive-field organization of different cell classes

In this study, we examined only those K, M, and P LGN cells that responded well to grating stimuli. The majority of these cells had standard center/surround receptive fields. We found that among the three cell classes, K cells had the largest r_c and r_s and the highest variability in these parameters. This description of K cells matches that reported for K cells in two other primate species, namely prosimian bush babies and New World simian marmosets, in which similar DOG models were used (Norton et al., 1988; Irvin et al., 1993; White et al., 2001). These data also are in agreement with results from our previous study in owl monkeys showing that K LGN cells have a lower spatial resolution than P cells and M cells (Xu et al., 2001a). Consistent with previous reports, we found that P cells in owl monkeys tend to have smaller center and surround radii, on average, than the M cells (Usrey & Reid, 2000; Xu et al., 2001a), although not statistically significant in our sample possibly due to sample size.

K cells were found to have lower average peak center and surround sensitivities than P and M cells. This result was expected

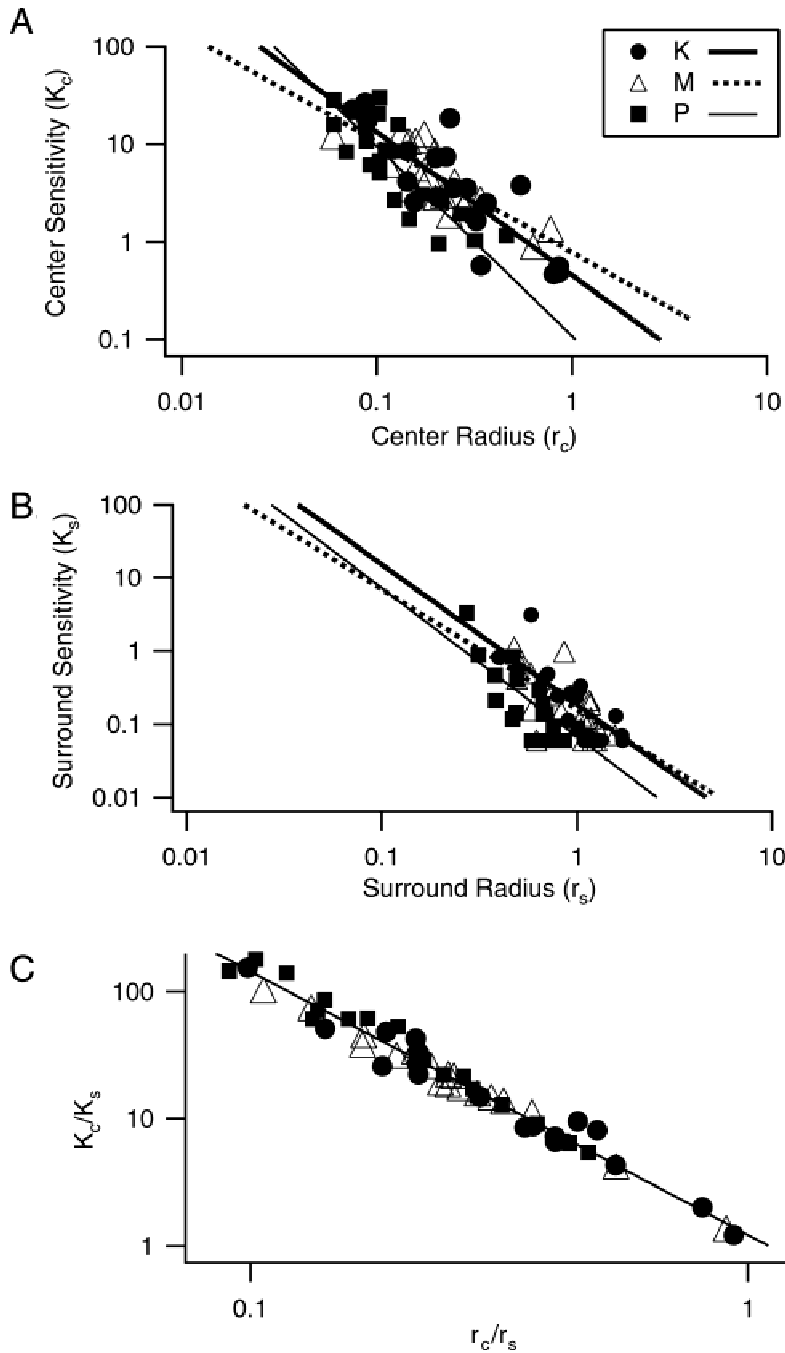


Fig. 2. Relationships between center and surround sensitivity in K, M, and P cells. (A) Center sensitivity (K_c) is plotted as a function of receptive-field center radius (r_c) on a double logarithmic scale. In this and subsequent figures, solid circles denote K cells, open triangles denote M cells, and filled squares denote P cells. The regression lines for the K (thick line), M (dotted line), and P (thin line) cells are defined as follows: K cells, $\log K_c = -1.46 * \log r_c - 0.34$ ($r^2 = 0.84$, $P < 0.0001$); M cells, $\log K_c = -1.13 * \log r_c - 0.11$ ($r^2 = 0.83$, $P < 0.0001$); and P cells, $\log K_c = -1.94 * \log r_c - 0.97$ ($r^2 = 0.81$, $P < 0.0001$). The overall regression line (not plotted) for the K, M, and P cells is defined as $\log K_c = -1.29 * \log r_c - 0.28$ ($r^2 = 0.65$, $P < 0.0001$). (B) Surround sensitivity (K_s) is plotted as a function of receptive-field surround radius (r_s) on a double logarithmic scale. The regression lines for the K (thick line), M (dotted line), and P (thin line) cells are defined as follows: K cells, $\log K_s = -1.92 * \log r_s - 0.74$ ($r^2 = 0.72$, $P = 0.0023$); M cells, $\log K_s = -1.64 * \log r_s - 0.80$ ($r^2 = 0.68$, $P = 0.0029$); and P cells, $\log K_s = -2.03 * \log r_s - 1.17$ ($r^2 = 0.77$, $P = 0.0002$). The overall regression line (not plotted) for the K, M, and P cells is defined as $\log K_s = -1.52 * \log r_s - 0.86$ ($r^2 = 0.41$, $P < 0.0001$). (C) Shows the decrease in sensitivity between center and surround within individual cells as a function of size increase from center to surround on a double logarithmic scale. The abscissa represents the log difference in radius between the center and the surround (r_c/r_s on a log scale = $\log r_c - \log r_s$). The ordinate represents the difference in (log) sensitivity between the center and the surround. The decrease in sensitivity is related to the size increase by the regression equation: $\log K_c/K_s = -2.07 * \log r_c/r_s + 0.087$ ($r^2 = 0.97$, $P < 0.0001$).

given that K cells had larger center and surround radii than P and M cells and given our demonstration that there is an inverse relationship between sensitivity and size for both center and surround for all cell classes. However, although the surround/center volume ratio remained similar across all three cell classes, K cells had significantly larger center and surround volumes than the M and P cells.

Owl monkey LGN cells have significantly lower K_c values than the values reported for macaque monkey retinal P and M cells (Croner & Kaplan, 1995), and also have lower values than those reported for K, M, and P LGN cells in marmosets using the same DOG model function (White et al., 2001). This could be explained by the fact that owl monkey LGN cells tend to show low overall

peak responses (Usrey & Reid, 2000; Xu et al., 2001a) and that the contrast sensitivity and gain of owl monkey LGN cells are markedly lower than those reported for macaque retinal ganglion cells and LGN cells (O'Keefe et al., 1998; Xu et al., 2001a). Why owl monkey LGN cells are less responsive is presently unclear unless they are more sensitive than other species to anesthetics or paralytics.

Cat X-, Y-, and W-cell receptive fields also have been fitted using a DOG model. In general, the relationships between center and surround for cat cells are similar to those described for primates. X cells have smaller center radii and higher center sensitivities than do Y cells. Center or surround sensitivity of X and Y cells decreases with increases in receptive-field center or surround radius (Linsenmeier et al., 1982). Like K cells, estimates

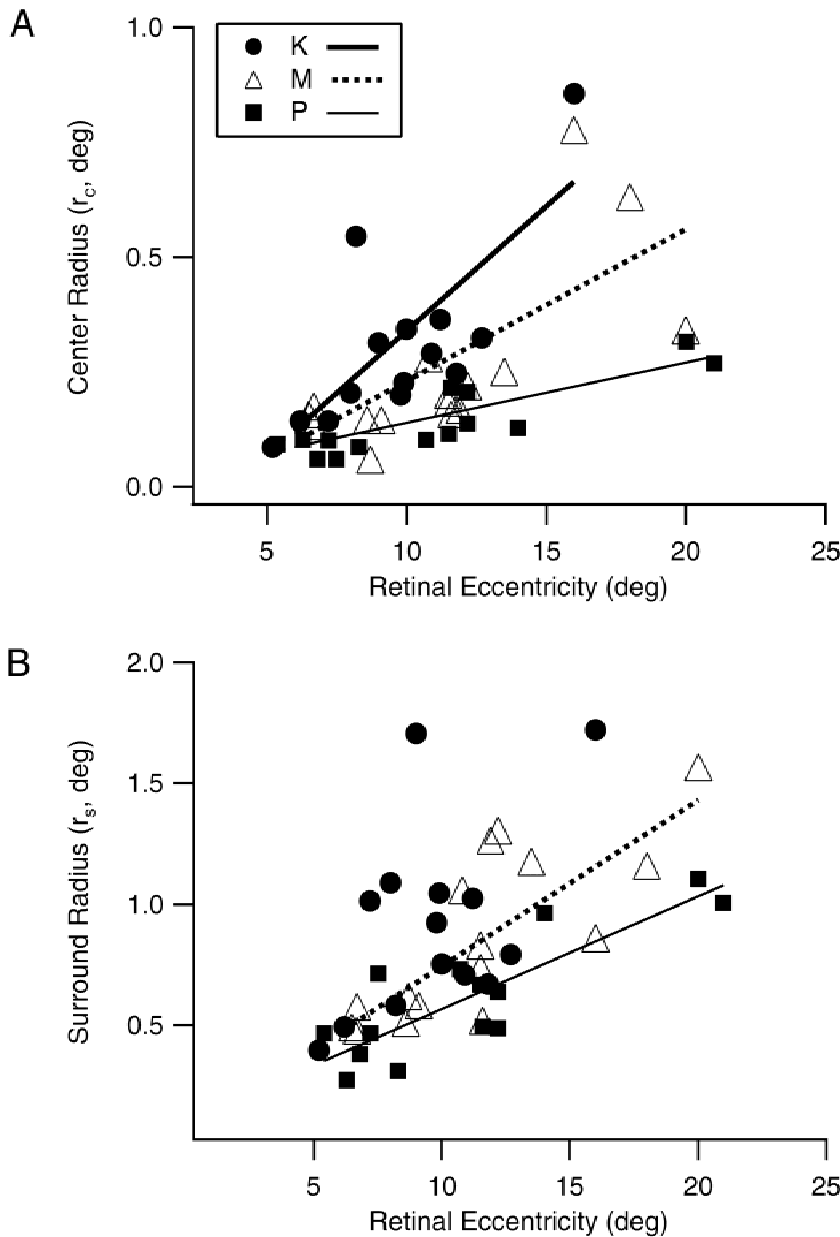


Fig. 3. Receptive-field size vs. retinal eccentricity. This figure includes a subset of the K (14), P (14), and M (16) cells for which receptive fields were carefully mapped. (A) Center size (r_c) is plotted as a function of retinal eccentricity. Symbols are as in Fig. 2. The regression lines are defined by the equations: K cells, $r_c = 0.063 * \text{Eccentricity} - 0.31$ ($r^2 = 0.59$, $P = 0.001$); M cells, $r_c = 0.034 * \text{Eccentricity} - 0.14$ ($r^2 = 0.51$, $P = 0.002$); and P cells, $r_c = 0.015 * \text{Eccentricity} - 0.017$ ($r^2 = 0.77$, $P < 0.0001$). (B) Surround size (r_s) is plotted as a function of retinal eccentricity. The regression lines are defined by the equations: K cells, $r_s = 0.067 * \text{Eccentricity} + 0.28$ ($r^2 = 0.24$, $P = 0.077$); the regression line is not shown due to $P > 0.05$; M cells, $r_s = 0.070 * \text{Eccentricity} + 0.058$ ($r^2 = 0.62$, $P < 0.0001$); and P cells, $r_s = 0.046 * \text{Eccentricity} + 0.12$ ($r^2 = 0.71$, $P < 0.0001$).

of the sensitivity of the center mechanism in W cells show that their sensitivity is significantly lower than the sensitivity of X or Y cells. Furthermore, W-cell center radii are significantly larger than those of X cells (Rowe & Cox, 1993).

Common center/surround relationships

Previous studies in cats, bush babies, macaque monkeys, and marmosets indicate that details of the relationship between center and surround control how retinal and LGN cells respond to visual stimuli and that some common principles exist for different cell classes across species. We confirmed these common center/surround relationships in owl monkey LGN cells.

First, in owl monkey LGN cells, receptive-field center and surround size tended to increase with increased eccentricity. K cells differed from P and M cells only in the overall degree of

variation in size. K cells in bush babies and marmosets also have relatively larger receptive-field centers than those of P and M cells at any given eccentricity, and the variability in K-cell center size is higher than that of P and M cells (Norton & Casagrande, 1982; Irvin et al., 1993; White et al., 2001). In owl monkeys, M cells had receptive-field center radii that were about twice the size of those of P cells. This is consistent with the reports for P and M cells in macaque retina (Croner & Kaplan, 1995). In cats, the center radii of X and Y cells increase with eccentricity, but center radii are generally two to three times larger for Y cells than for X cells at a given eccentricity (Linsenmeier et al., 1982). For cat tonic W cells, there is a tendency for center radii to increase with eccentricity, but there is no tendency for the radii of phasic W cells to increase with eccentricity (Rowe & Cox, 1993; Troy et al., 1995).

Second, we found that all K, M, and P LGN cells showed decreased sensitivity with increasing center or surround size. If the

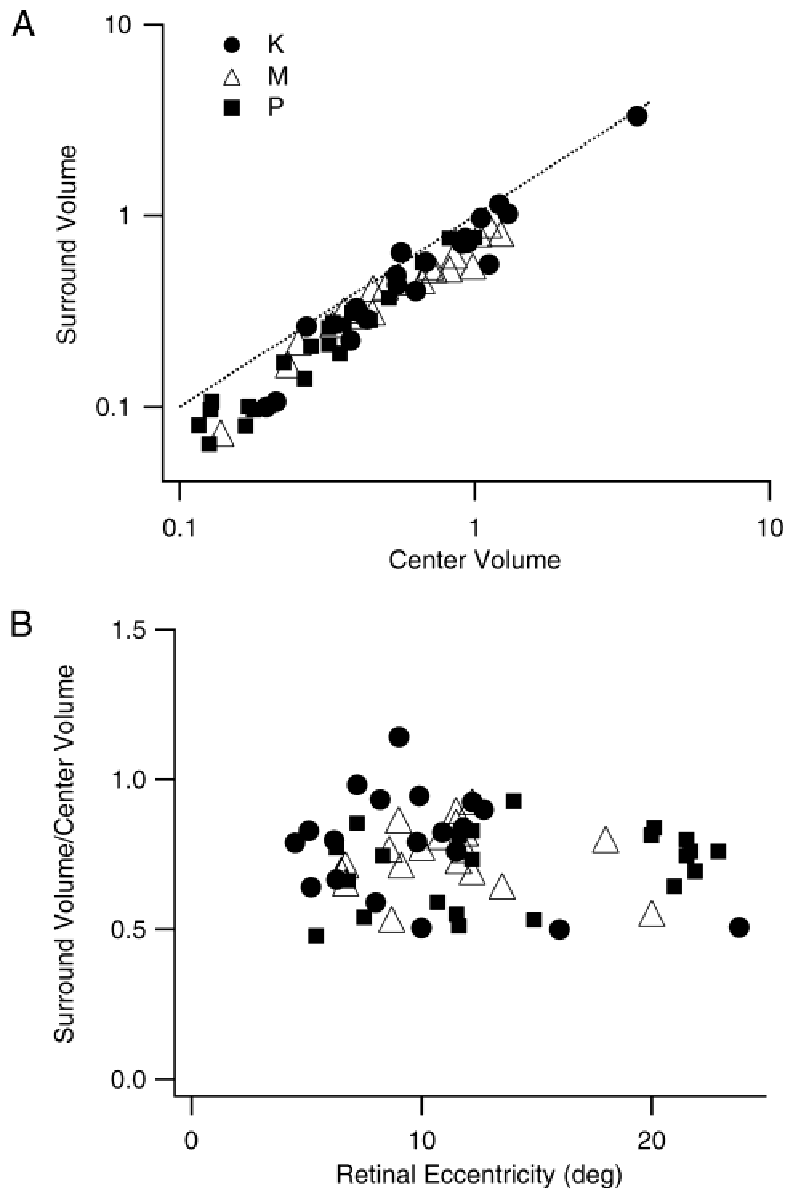


Fig. 4. Relationship between center and surround volume. (A) Surround volume plotted as a function of center volume on a double logarithmic scale. The regression line (not shown) is defined by the equation: Surround Volume = $1.08 * \text{Center Volume} + 0.093$ ($r^2 = 0.96$, $P < 0.0001$). The dotted line in the figure indicates a 1:1 relationship. Only one cell (a K cell) lies above the 1:1 relationship line, showing that its surround volume is larger than its center volume. (B) Center volume/surround volume plotted as a function of retinal eccentricity. There is no clear relationship between the ratios of center volume/surround volume and eccentricity.

center or surround sensitivity is inversely proportional to center or surround area, sensitivity plotted against receptive-field radius on a double logarithmic scale produces a regression line with a slope of -2 . The fact that the slope of the regression line is less than -2 implies that for owl monkey LGN cells, sensitivity for the center and surround does not decrease in direct proportion to the size of receptive-field area (see also Linsenmeier et al., 1982; Irvin et al., 1993). This sensitivity reduction also held between center and surround within individual cells. The tight regression (slope close to -2) suggests that the sensitivity decrease between center and surround within individual cells is closely related to the size increase from center to surround. Similar relationships have been seen in both cats and bush babies (Linsenmeier et al., 1982; Irvin et al., 1993).

Finally, there is a strong relationship between the center and surround volume across all cell classes in owl monkeys as well as other species. Center volumes for most K, M, and P cells are larger than their surround volumes (Croner & Kaplan, 1995; Irvin et al.,

1993; White et al., 2001; present study). In bush babies about 80% of LGN cells including some K, M, and P cells have larger center volumes than surround volumes (Irvin et al., 1993). All the P and M retinal cells in macaque monkeys have larger center volumes than surround volumes (Croner & Kaplan, 1995). Almost no cat retinal ganglion cells are found to have a larger surround volume than a center volume (Enroth-Cugell & Robson, 1966; Linsenmeier et al., 1982). Having a higher center volume than a surround volume is consistent with the fact that most cells respond to diffuse illumination of both the center and surround with the sign of the center, because the center mechanism is stronger than the surround mechanism.

The role of K cells

Although P and M cells have been studied extensively and hypotheses proffered as to their functions, the roles of K cells in vision are still unclear (Casagrande, 1994, 1999; Hendry & Reid,

2000). Our previous findings in owl monkey and comparable data in bush babies suggest that many K cells exhibit spatial and temporal resolution values in the range that would allow these cells to contribute to conventional aspects of spatial and temporal vision (Xu et al., 2001a). This is consistent with modeling results of receptive-field organization of K, M, and P cells in this study.

One important result from the present modeling study is that K cells had the largest r_c and r_s among the three cell classes. Studies in cat retina have shown that ganglion cells with large centers show more rapid light adaptation (Enroth-Cugell & Shapley, 1973; Harding & Enroth-Cugell, 1978). In owl monkeys, therefore, K cells would be expected to adapt quickly, which might be an advantage for these nocturnal animals. This explanation, however, also would hold for nonchromatically selective K cells in diurnal simians such as the marmoset, since K cells in marmosets also have larger receptive-field centers and the majority (80%) of K cells in marmosets are not selective for wavelength (White et al., 2001). Regardless, it is clear that more information about K-cell properties in several primate species will be needed before testable hypotheses about their role or roles in vision can be developed.

Acknowledgments

We thank Dr. Jamie Boyd and Patrick Pratumrat for help with data collection and model fitting. We also thank Drs. Jeffrey Schall, John Allison, Gyula Sáry, and Yuri Shostak, Jennifer Ichida, David Royal, Julia Mavity-Hudson, and Kelly Lusk for helpful comments on the manuscript. This research was supported by grants EY01778 (V.A.C.), EY03778 (A.B.B.), and core grants EY08126 and HD15052.

References

- CASAGRANDE, V.A. (1994). A third parallel visual pathway to primate area V1. *Trends in Neurosciences* **17**, 305–310.
- CASAGRANDE, V.A. (1999). The mystery of the visual system K pathway. *Journal of Physiology* **517**, 630.
- CASAGRANDE, V.A. & KAAS, J.H. (1994). The afferent, intrinsic, and efferent connections of primary visual cortex. In *Cerebral Cortex*, vol. 10, Primary Visual Cortex of Primates, ed. PETERS, A. & ROCKLAND, K.S., pp. 201–259. Plenum Press, New York.
- CASAGRANDE, V.A. & NORTON, T.T. (1991). The lateral geniculate nucleus: A review of its physiology and function. In *The Neural Basis of Visual Function*, ed. LEVENTHAL, A.G., Volume 4: *Vision and Visual Dysfunction* series, ed. CRONLEY-DILLON, J.R., pp. 41–84. London: MacMillan Press.
- CRONER, L.J. & KAPLAN, E. (1995). Receptive fields of P and M ganglion cells across the primate retina. *Vision Research* **35**, 7–24.
- DERRINGTON, A.M. & LENNIE, P. (1984). Spatial and temporal contrast sensitivities of neurons in lateral geniculate nucleus of macaque. *Journal of Physiology* **357**, 219–240.
- ENROTH-CUGELL, C. & ROBSON, J. (1966). The contrast sensitivity of retinal ganglion cells of the cat. *Journal of Physiology* **187**, 517–552.
- ENROTH-CUGELL, C. & SHAPLEY, R.M. (1973). Flux, not retinal illumination, is what cat retinal ganglion cells really care about. *Journal of Physiology* **233**, 311–326.
- HARDING, T.H. & ENROTH-CUGELL, C. (1978). Absolute dark sensitivity and center size in cat retinal ganglion cells. *Brain Research* **153**, 157–162.
- HENDRY, S.H. & REID, R.C. (2000). The koniocellular pathway in primate vision. *Annual Review of Neuroscience* **23**, 127–153.
- IRVIN, G.E., CASAGRANDE, V.A. & NORTON, T.T. (1993). Center/surround relationships of magnocellular, parvocellular, and koniocellular relay cells in primate lateral geniculate nucleus. *Visual Neuroscience* **10**, 363–373.
- JACOBS, G.H., DEEGAN, J.F., NEITZ, J., CROGNALE, M.A. & NEITZ, M. (1993). Photopigments and color vision in the nocturnal monkey, *Aotus*. *Vision Research* **33**, 773–783.
- KREMERS, J. & WEISS, S. (1997). Receptive field dimensions of lateral geniculate cells in the common marmoset (*Callithrix jacchus*). *Vision Research* **37**, 2171–2181.
- LINSENMEIER, R.A., FRISHMAN, L.J., JAKIELA, H.G. & ENROTH-CUGELL, C. (1982). Receptive field properties of X and Y cells in the cat retina derived from contrast sensitivity measurements. *Vision Research* **22**, 1173–1183.
- MARTIN, P.R., WHITE, A.J., GOODCHILD, A.K., WILDER, H.D. & SEFTON, A.E. (1997). Evidence that blue-on cells are part of the third geniculocortical pathway in primates. *European Journal of Neuroscience* **9**, 1536–1541.
- NORTON, T.T. & CASAGRANDE, V.A. (1982). Laminar organization of receptive-field properties in lateral geniculate nucleus of bush baby (*Galago crassicaudatus*). *Journal of Neurophysiology* **47**, 715–741.
- NORTON, T.T., CASAGRANDE, V.A., IRVIN, G.E., SESMA, M.A. & PETRY, H.M. (1988). Contrast-sensitivity functions of W-, X-, and Y-like relay cells in the lateral geniculate nucleus of bush baby, *Galago crassicaudatus*. *Journal of Neurophysiology* **59**, 1639–1656.
- NORTON, T.T., HOLDEFER, R.N. & GODWIN, D.W. (1989). Effects of bicuculline on receptive field center sensitivity of relay cells in the lateral geniculate nucleus. *Brain Research* **488**, 348–352.
- O'KEEFE, L.P., LEVITT, J.B., KIPPER, D.C., SHAPLEY, R.M. & MOVSHON, J.A. (1998). Functional organization of owl monkey lateral geniculate nucleus and visual cortex. *Journal of Neurophysiology* **80**, 594–609.
- RODIECK, R.W. (1965). Quantitative analysis of cat retinal ganglion cell response to visual stimuli. *Vision Research* **5**, 583–601.
- ROWE, M.H. & COX, J.F. (1993). Spatial receptive-field structure of cat retinal W cells. *Visual Neuroscience* **10**, 765–779.
- SO, Y.T. & SHAPLEY, R. (1981). Spatial tuning of cells in and around lateral geniculate nucleus of the cat: X and Y relay cells and perigeniculate interneurons. *Journal of Neurophysiology* **45**, 107–120.
- TROY, J.B., SCHWEITZER-TONG, D.E. & ENROTH-CUGELL, C. (1995). Receptive-field properties of Q retinal ganglion cells of the cat. *Visual Neuroscience* **12**, 285–300.
- USREY, W.M. & REID, R.C. (2000). Visual physiology of the lateral geniculate nucleus in two species of New World monkey: *Saimiri sciureus* and *Aotus trivirgatus*. *Journal of Physiology* **523**, 755–769.
- WHITE, A.J., WILDER, H.D., GOODCHILD, A.K., SEFTON, A.J. & MARTIN, P.R. (1998). Segregation of receptive field properties in the lateral geniculate nucleus of a New-World monkey, the marmoset *Callithrix jacchus*. *Journal of Neurophysiology* **80**, 2063–2076.
- WHITE, A.J., SOLOMON, S.G. & MARTIN, P.R. (2001). Spatial properties of koniocellular cells in the lateral geniculate nucleus of the marmoset *Callithrix jacchus*. *Journal of Physiology* **533**, 519–535.
- WIKLER, K.C. & RAKIC, P. (1990). Distribution of photoreceptor subtypes in the retina of diurnal and nocturnal primates. *Journal of Neuroscience* **10**, 3390–3401.
- XU, X., ICHIDA, J.M., ALLISON, J.D., BOYD, J.D., BONDS, A.B. & CASAGRANDE, V.A. (2001a). A comparison of koniocellular, magnocellular, and parvocellular receptive field properties in the lateral geniculate nucleus of the owl monkey (*Aotus trivirgatus*). *Journal of Physiology* **531**, 203–218.
- XU, X., PRATUMRAT, P., BONDS, A.B. & CASAGRANDE, V.A. (2001b). Center/surround relationships of koniocellular (K), magnocellular (M), and parvocellular cells in lateral geniculate nucleus (LGN) of the owl monkey. *Society for Neuroscience Abstracts* **31**, Program No. 723.16.
- XU, X., ICHIDA, J., SHOSTAK, Y., BONDS, A.B. & CASAGRANDE, V.A. (2002). Are primate lateral geniculate nucleus (LGN) cells really sensitive to orientation or direction? *Visual Neuroscience* **19**, 97–108.